

## Tagged-particle motion in viscous glycerol: Diffusion-relaxation crossover

J. Wuttke,<sup>1</sup> I. Chang,<sup>2</sup> O. G. Randl,<sup>3</sup> F. Fajara,<sup>4</sup> and W. Petry<sup>1</sup>

<sup>1</sup>*Physik-Department, Technische Universität München, 85747 Garching, Germany*

<sup>2</sup>*Institut für Physikalische Chemie, Universität Mainz, 55 099 Mainz, Germany*

<sup>3</sup>*Institut Laue-Langevin, 38 042 Grenoble, France*

<sup>4</sup>*Experimentalphysik III, Universität Dortmund, 44 221 Dortmund, Germany*

(Received 21 May 1996)

Incoherent neutron-backscattering and field gradient NMR are combined to measure the self-correlation function of protons in glycerol. Extensive simulations reveal and delimit systematic effects of multiple scattering. At microscopic wave numbers, tagged-particle motion couples strongly to structural relaxation. Between 1 and 0.1 Å<sup>-1</sup> a crossover to diffusional motion is observed: quasielastic stretching diminishes and the wave-number dependence of the mean relaxation time approaches  $q^{-2}$ . [S1063-651X(96)04811-8]

PACS number(s): 64.70.Pf, 66.10.-x, 61.12.-q, 76.60.Lz

### I. INTRODUCTION

The motion of a tagged particle in a dense liquid is easily understood in the two limiting cases of large or small wave numbers [1]. For very large  $q$ , one expects to see the thermal motion of a free particle. In the limit  $q \rightarrow 0$ , on the other hand, the particle motion can be described as Brownian diffusion, leading to an exponential decay of time correlations [2,3]. In the intermediate range where  $q^{-1}$  is of the order of interparticle distances, no universal law can be given. Until now, only in a small number of simple liquids has the full crossing over from the free particle to the diffusion limit been experimentally covered and theoretically understood [3–5].

In the present paper, we investigate tagged-particle motion in a supercooled, glass forming liquid. We juxtapose NMR field gradient echo measurements and quasielastic incoherent neutron scattering (INS), which allows us to cover an asymptotically small and an intermediate range in  $q$ . In a hydrogen-rich sample, both techniques can be employed to observe essentially the same self-correlation function  $S(q, t)$  of protons.

As a model system we choose glycerol [C<sub>3</sub>H<sub>5</sub>(OH)<sub>3</sub>,  $T_g = 185$  K,  $T_m = 291$  K]. With its ability to form multiple hydrogen bonds, glycerol is representative for systems with a weak network structure. Its glass transition dynamics has already been studied by an impressive variety of experimental methods [6]. Recent light- and neutron-scattering experiments on glycerol [7–9] have shown that atomic correlation functions decay essentially in two steps, associated with vibrations and structural  $\alpha$  relaxation, respectively; the intermediate step of fast  $\beta$  relaxation, predicted by mode-coupling theory [10] and observed in a number of fragile liquids [11,12] is quite weak in glycerol. This allows us to study the coupling between one-particle motion and structural relaxation on microscopic time scales down to a few picoseconds without a need to consider faster processes in our analysis.

### II. MEASURING SELF-CORRELATIONS

The self-correlation of protons in a viscous medium can be measured with NMR stimulated echo in a static magnetic

field gradient [13]. Using a  $(\pi/2) - \tau - (\pi/2) - t - (\pi/2) - \tau$  echo three-pulse sequence (with evolution time  $\tau$  and diffusion time  $t \gg \tau$ ) the echo height is proportional to the intermediate self-correlation function

$$\Phi_q(t) = \frac{1}{N} \sum_j \langle e^{i\mathbf{q} \cdot \mathbf{R}_j(0)} e^{-i\mathbf{q} \cdot \mathbf{R}_j(t)} \rangle, \quad (1)$$

with the generalized scattering vector  $\mathbf{q} = \tau \gamma \mathbf{g}$  (gyromagnetic ratio  $\gamma$ , magnetic-field gradient  $\mathbf{g}$ ). Measurements were performed on a homemade spectrometer at Mainz University. In favorable cases [14] wave numbers up to  $10^{-2}$  Å<sup>-1</sup> can be reached, using ultrahigh static field gradients of up to 200 T/m. In the present study field gradients between 44 and 71 T/m and evolution time  $\tau$  between 20 and 610  $\mu$ s gave access to wave numbers between  $2.35 \times 10^{-5}$  and  $1.82 \times 10^{-3}$  Å<sup>-1</sup>.

In contrast to NMR, neutron scattering cannot selectively observe a single isotope within a chemically complex sample. Nevertheless, in the case of hydrogen-rich organic matter, the total cross section is largely dominated by incoherent scattering from the H nuclei. In order to concentrate on the motion of the molecule's main chain and for consistency with earlier measurements on glycerol [7,8], protons in the OH groups were exchanged against deuterons. Even so, scattering from C<sub>3</sub>H<sub>5</sub>(OD)<sub>3</sub> is about 90% incoherent. The NMR experiment was performed on ordinary glycerol C<sub>3</sub>H<sub>5</sub>(OH)<sub>3</sub>. Since intramolecular modes of glycerol are invisible in the time and wave-number range of field gradient NMR, we still can equate the self-correlations measured by both methods. Deuterating the OH groups has also a direct impact on the molecule's mobility, but from viscosity measurements the isotope effect is known not to exceed 10% [15], so that it will have no consequences for the conclusions reached in this work.

Neutron scattering experiments were performed on the backscattering spectrometer IN10 at the Institut Laue-Langevin. Different configurations of the instrument were used to cover wave numbers between 0.11 and 3.7 Å<sup>-1</sup>, but outside the range 0.19–1.9 Å<sup>-1</sup> count rates were too low and the resolution function too fuzzy to allow for a quantitative data analysis. The temperature range 254–413 K was

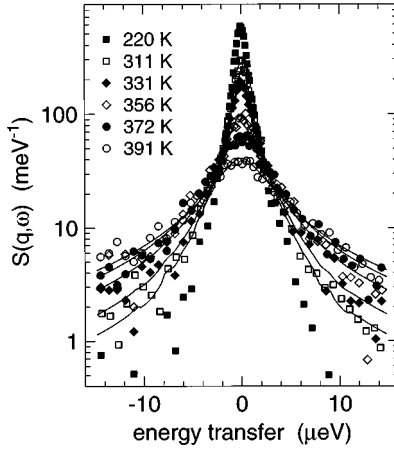


FIG. 1. Incoherent neutron-scattering law  $S(q, \omega)$  of glycerol  $C_3H_5(OD)_3$  at  $q = 0.50 \text{ \AA}^{-1}$ . The measurement at 220 K yields the instrumental resolution function. The quasielastic scattering in the viscous liquid is fitted with the Kohlrausch function with a fixed exponent  $\beta = 0.60$ . Hitherto, logarithmic intensity scales have seldom been employed in the presentation of neutron-backscattering data.

the same as in the NMR experiment. Raw data were corrected for background scattering and normalized to the elastic intensity measured below the glass transition. Some spectra are shown in Fig. 1. After Fourier transformation and deconvolution of the instrumental resolution function, one obtains the intermediate scattering law (1).

### III. SCALING ANALYSIS

The free spectral range of a neutron-backscattering spectrometer hardly ever permits one to determine from a single measurement the line shape of a complex relaxational process. Much more can be learned from the experimental data if it is possible to condense them by some kind of scaling procedure.

We shall analyze the self-correlation measured by NMR and INS in close analogy to the case of coherent neutron scattering (CNS). Coherent scattering from structural relaxation has been studied in a recent spin-echo experiment [16] on perdeuterated glycerol around the structure factor maximum ( $q = 1.44 \pm 0.13 \text{ \AA}^{-1}$ ). We found that the intermediate scattering function  $\Phi_q^{\text{coh}}(t)$  could be written in the scaling form

$$\Phi_q(t) = f_q(T) F_q(t/\tau(T)), \quad (2)$$

where the characteristic time  $\tau$  follows over more than three decades the temperature dependence of viscosity,

$$\tau \propto \eta(T)/T, \quad (3)$$

the line shape of  $F_q(\tilde{t})$  varies only weakly with temperature, and the master curve could be fitted over four decades in reduced time  $\tilde{t}$  by the stretched exponential of Kohlrausch,

$$F_q(\tilde{t}) = \exp[-(\tilde{t}/\tilde{\tau}_q)^{\beta_q}]. \quad (4)$$

The exponent  $\beta_q^{\text{coh}} \approx 0.7$  was found to depend not or only weakly on temperature. Similar scaling properties had been

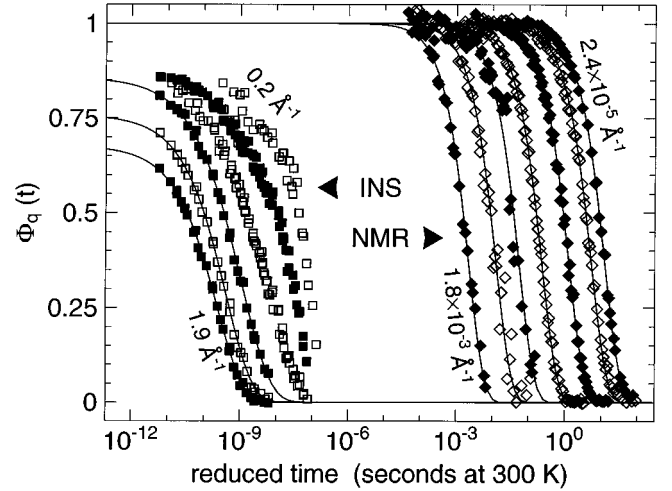


FIG. 2. Self-correlation function  $\Phi_q(\tilde{t})$ , deduced from incoherent neutron scattering (INS) and field gradient NMR measurements, as a function of reduced time  $\tilde{t} = t[\eta(T_0)/T_0]/[\eta(T)/T]$  with arbitrary normalization  $T_0 = 300 \text{ K}$ . The master curves are combined from measurements between 270 and 413 K. NMR data are fitted with an exponential law, large-angle INS data with a Kohlrausch function. The INS data are shown in more detail in Fig. 3.

found in previous studies of other viscous liquids [17–19]. While the precision of our spin-echo data allowed us to correct for the temperature dependence of the Debye-Waller factor, in the present INS analysis this weak effect is neglected, taking  $f_q(T)$  as usual to be  $T$  independent. In the  $q$  range of NMR, one has anyhow  $f_q(T) = 1$ .

Master curves are obtained by superimposing the  $\Phi_q(\tilde{t})$  as a function of reduced time  $\tilde{t} = t/[\tau(T)/\tau(T_0)]$ , taken from published viscosity measurements [20]; absolute units were set by arbitrarily choosing  $T_0 = 300 \text{ K}$ . For neighboring temperatures, the data do satisfactorily coincide. A majority of so obtained master curves is shown in Fig. 2.

As expected for ordinary diffusion, the NMR data follow an exponential law

$$\Phi_q(\tilde{t}) = \exp(-\tilde{t}/\tilde{\tau}_q). \quad (5)$$

For  $q \geq 0.5 \text{ \AA}^{-1}$ , on the other hand, the INS data are well described by the Kohlrausch function (4), as expected for any microscopic correlator that couples strongly to structural relaxations. Somewhere between  $2 \times 10^{-3} \text{ \AA}^{-1}$  and  $0.5 \text{ \AA}^{-1}$ , the self-correlation function must cross over from diffusionlike to relaxationlike behavior. As we will see, there are some indications that this crossing over falls at least partly in the wave-number range  $0.2\text{--}0.5 \text{ \AA}^{-1}$  covered by our INS experiment.

In Fig. 3, the neutron-scattering data are analyzed in more detail. We first determined an estimate of the mean relaxation time

$$\langle \tau_q \rangle = \int_0^\infty dt F_q(t) = \beta^{-1} \Gamma(\beta^{-1}) \tau_q \quad (6)$$

and then restricted subsequent fits to the time range  $t > \langle \tau_q \rangle / 100$ . For  $q > 0.5 \text{ \AA}^{-1}$  one verifies again that within statistical accuracy the master curves are correctly described by (4). For  $q = 1.2\text{--}1.9 \text{ \AA}^{-1}$ , a stretching exponent  $\beta = 0.61 \pm 0.01$  is found and for  $q = 0.87 \text{ \AA}^{-1}$  a lower value

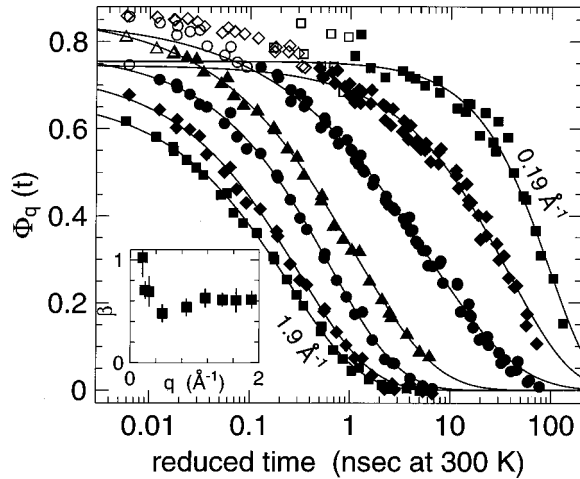


FIG. 3. INS master curves as in Fig. 2, for wave numbers  $q=0.19, 0.29, 0.50, 0.87, 1.2, 1.6,$  and  $1.9 \text{ \AA}^{-1}$ . For small wave numbers and short reduced times the data are severely affected by multiple scattering; in particular the amplitudes do not show the  $q$  dependence expected for a harmonic Debye-Waller factor. Data points with  $t < \langle \tau_q \rangle / 100$ , plotted as open symbols, are therefore excluded from the quantitative analysis. Solid lines are Kohlrausch fits for  $t > \langle \tau_q \rangle / 100$ . The inset shows the stretching exponent as a function of  $q$ ; compare the discussion in the text.

of 0.54. For  $q \leq 0.3 \text{ \AA}^{-1}$ , on the other hand, the master curves can be fitted by a Kohlrausch function only if short-time data are systematically excluded, and the stretching exponent  $\beta_q$  depends considerably on the modalities of fitting, while for  $q > 0.5 \text{ \AA}^{-1}$  its value is quite stable. With this reservation in mind, we note that the relaxational stretching diminishes strongly with decreasing wave number, approaching almost single exponential decay for  $q = 0.19 \text{ \AA}^{-1}$ .

In Fig. 4, the mean relaxation time  $\langle \tau_q \rangle$  is plotted as a function of the wave number  $q$ . As expected for normal diffusion, the NMR data obey

$$\langle \tau_q \rangle = D^{-1} q^{-2}. \quad (7)$$

One may anticipate that this power law continues to hold in the experimental wave-number gap above  $2 \times 10^{-3} \text{ \AA}^{-1}$ . In fact, if (7) is extrapolated over more than two decades in  $q$ , up to about 0.2 or 0.3  $\text{\AA}^{-1}$ , it merges, within a factor 2, with the relaxation times measured by neutron scattering. Towards larger wave numbers, however, the extrapolation cannot be continued: within the INS data range, the  $q$  dependence of  $\langle \tau_q \rangle$  is clearly steeper than  $q^{-2}$ .

So both the time dependence of the master curves  $\Phi_q(\tilde{t})$  and the wave-number dependence of the mean relaxation time  $\langle \tau_q \rangle$  indicate that up to at least  $0.1 \text{ \AA}^{-1}$  self-diffusion is correctly described by the hydrodynamic limit and that the crossover to stretched exponential relaxation is observed within the experimental window of INS.

Any such interpretation, however, has to rely critically on neutrons scattered with rather small wave-number transfers. In previous experiments on amorphous samples [8,21] we have systematically discarded all small-angle data because, as is well known, inelastic scattering at small angles is most severely affected by multiple scattering. Therefore, we first

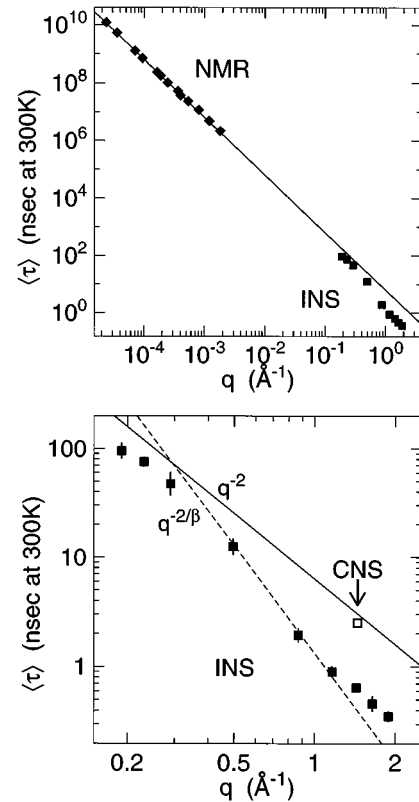


FIG. 4. Mean relaxation time  $\langle \tau_q \rangle$  as a function of  $q$ . The solid line is a fit  $\tau = D^{-1} q^{-2}$  to the NMR data. In the bottom plot, the INS data are enlarged and the relaxation time measured by coherent neutron scattering (CNS) at the structure factor maximum is shown for comparison. The broken line is a fit to the INS data with a power law  $q^{-2\beta}$  ( $\beta=0.61$ ), as suggested by recent work on polymers; the solid line is exactly the same as in the top plot.

have to clarify to what extent our results might be artifacts due to the use of a relatively thick sample (about 20% scattering).

#### IV. MULTIPLE SCATTERING

In order to estimate possible influences of multiple scattering we performed an extensive model calculation. The scattering experiment was simulated with a Monte Carlo program based on MSCAT by Bishop and Copley [22]. For the backscattering situation in which energy transfers are much smaller than the incoming neutron energy, central parts of the algorithm had to be rewritten.

Any multiple-scattering simulation requires input of the ideal scattering law  $S^*(q, \omega)$  over an extended  $q\omega$  range. Since there is no closed theoretical expression for  $S^*(q, \omega)$  of glycerol, we had to use an idealized model. In order to keep our model as simple as possible, we concentrated on structural relaxation, neglecting any faster process that cannot be resolved on IN10. We constructed  $S^*(q, \omega)$  by numerical Fourier transform of a Kohlrausch curve with an invariant stretching exponent  $\beta=0.55$ . Relaxation times were assumed to scale over the full wave-number range as  $\tau_q \propto q^2$ ; the absolute time scale was varied over four decades, corresponding to nine different temperatures. One more temperature was needed to generate the resolution function.

Sample geometry and energy mesh were adopted from the IN10 setup.

Simulated spectra were then analyzed along the same lines as our experimental data. Figure 5 shows the Fourier deconvoluted, rescaled  $\Phi_q(\tilde{t})$  for a 5% and a 20% scatterer, for the smallest and the highest wave number used on IN10. In all cases the data fall onto master curves, slight deviations appearing only at the lowest temperature, corresponding to times  $t \lesssim \langle \tau_q \rangle / 100$ . All curves are well fitted by the Kohlrausch function (4). The stretching exponent, however, shows more or less pronounced deviations from the input value 0.55 and a strong wave number dependence: For large  $q > 1 \text{ \AA}^{-1}$  the deviation from the input  $\beta$  is in no case larger than 0.05, while there is an extended minimum at smaller scattering angles, around  $q = 0.2 \text{ \AA}^{-1}$ , where  $\beta_q$  drops to 0.48 for the 5% and to 0.41 for the 20% scatterer. For even smaller wave numbers  $\beta_q$  increases again.

Qualitatively, these findings can be explained as follows. For an isotropic scatterer, more than 85% of all scattering processes involve angles  $2\theta > 45^\circ$ , corresponding to wave numbers  $q > 0.74 \text{ \AA}^{-1}$ . For scattering angles between  $45^\circ$  and  $180^\circ$ ,  $q$  varies by less than a factor 3. Thus multiple scattering is dominated by an almost isotropic contribution from large-angle scattering processes. At large wave numbers, these processes corrupt absolute intensities but do not change spectral line shapes very much. At smaller wave numbers, on the other hand, the scattering law responsible for single scattering is quite different from the isotropic background, so that even a comparatively small contribution of 5% double scattering can considerably increase the stretching of the quasielastic spectrum. Finally, at very small wave numbers  $q \lesssim 0.2 \text{ \AA}^{-1}$  and low temperatures, the line-width of  $S^*(q, \omega)$  is much smaller than the instrumental resolution. The quasielastic spectrum is then given by the multiple-scattering contribution alone. This explains also the paradoxical result that for  $q \lesssim 0.15 \text{ \AA}^{-1}$ , the thick sample shows less stretching than the thin one. Note that these effects are the inevitable consequence of the strong wave-number dependence of  $S^*(q, \omega)$  and that not even the use of a rather thin sample can prevent a considerable systematic error in the determination of  $\beta$ .

In contrast to the spectral line shape, the mean relaxation time  $\langle \tau_q \rangle$  is only weakly affected by multiple scattering. Even for the 20% scatterer, it follows over the full wave-number range the  $\tau_q \propto q^{-2}$  law; input values and fit results coincide within 10%. Again, a simple qualitative explanation can be given: The mean relaxation time, given by the integral (6), depends ultimately on the value of the scattering law at  $\omega = 0$ ,

$$\langle \tau_q \rangle = S(q, \omega = 0) / f_q(T). \quad (8)$$

In our model,  $S(q, \omega \rightarrow 0)$  is sharply peaked for small  $q$ , so that the flatter background from large-angle multiple scattering does not influence the value of  $\langle \tau_q \rangle$ . Therefore, even if spectral line shapes are severely damaged by multiple scattering, quasielastic scattering experiments do still permit a reliable determination of the mean relaxation time  $\langle \tau_q \rangle$ .

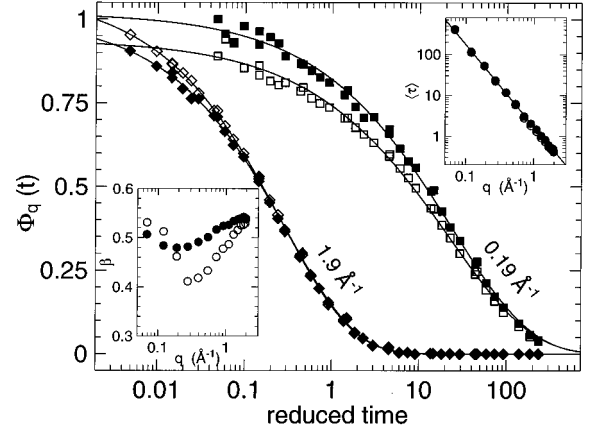


FIG. 5. Simulation of quasielastic incoherent neutron scattering for a 5% scatterer (full symbols) and a 20% scatterer (open symbols) under IN10 conditions. The master curves were obtained along the same lines as the experimental curves in Figs. 2 and 3; data points with  $t < \langle \tau_q \rangle / 1000$  are not shown. Solid lines are Kohlrausch fits; the insets show stretching exponents and mean relaxation times. The relaxation times follow within 10% the  $q^{-2}$  behavior chosen on input, whereas the stretching exponent is severely affected by multiple scattering. Its  $q$  dependence can be understood from the simple considerations outlined in Sec. IV. The amount by which  $\beta_q$  falls below the input value 0.55 can be reduced by about one-third if the fits are restricted to  $t > \langle \tau_q \rangle / 100$ .

## V. DISCUSSION

After delimiting the effects of multiple scattering we can now proceed with a critical discussion of our data. We consider first the line shapes of the master curves  $\Phi_q(\tilde{t})$ . For  $q \geq 1 \text{ \AA}^{-1}$ , the Kohlrausch fits yielded a rather constant stretching exponent  $\beta = 0.61 \pm 0.01$  (Fig. 3, inset). Our Monte Carlo simulation suggests that this comes close to the real value, which may be some 0.01 higher. For intermediate wave numbers  $q = 0.87$  and  $0.50 \text{ \AA}^{-1}$  the fitted exponent  $\beta$  drops by more than 0.1. This wave-number dependence corresponds exactly to what we have seen in the simulation and can safely be attributed to multiple scattering.

Turning now to small wave numbers, two anomalies are observed: The full master curves cannot be described by Kohlrausch functions and if the fit is restricted to times  $t > \langle \tau_q \rangle / 100$  the resulting exponent  $\beta_q$  tends towards 1. To understand this behavior we go back to the original spectra measured in the energy domain. In Fig. 6(a) typical low-temperature data are shown: While structural relaxation is well resolved at  $q = 1.4 \text{ \AA}^{-1}$ , it cannot be observed at  $0.19 \text{ \AA}^{-1}$ . The broad wings of the measured spectrum can be fully ascribed to large-angle multiple scattering. Consequently, all small-angle, low-temperature data are systematically discarded from our quantitative analysis by restricting the fits to sufficiently long reduced times.

In Fig. 6(b) the opposite limit is shown: At high temperatures, the quasielastic broadening is well resolved at  $q = 0.19 \text{ \AA}^{-1}$ , while at  $1.4 \text{ \AA}^{-1}$  it is so strong that within the given energy range of IN10 it appears only as a flat background. In such a situation, multiple scattering can only somewhat lower the effective stretching exponent; it cannot account for  $\beta$  rising above the value measured at large

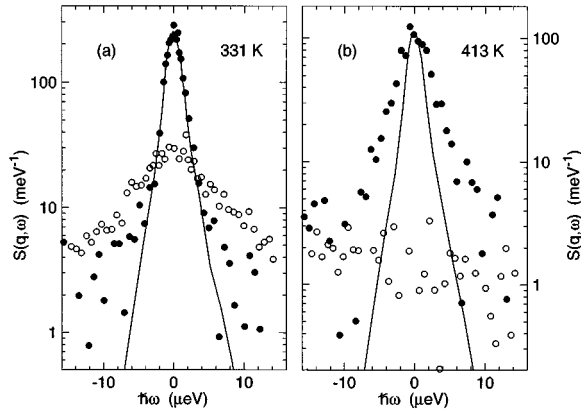


FIG. 6. Incoherent neutron-scattering law  $S(q, \omega)$  at  $q=0.19$  (●) and  $1.4 \text{ \AA}^{-1}$  (○). The solid line shows the resolution function, measured at  $0.19 \text{ \AA}^{-1}$  and rescaled to the peak of the quasielastic scan. (a) At 331 K and  $0.19 \text{ \AA}^{-1}$ , structural relaxation cannot be resolved. The effective broadening in the wings is entirely due to multiple large-angle scattering. (b) At 413 K, on the other hand, large-angle scattering is so greatly broadened that it appears within the energy window of IN10 as a flat background. Structural relaxation can be well resolved at  $0.19 \text{ \AA}^{-1}$ : Small-angle, high-temperature data are not seriously damaged by multiple scattering.

angles. Experimental artifacts cannot explain the observed variation of  $\Phi_q(\bar{t})$ .

At this point, however, we must recall that master curves at different values of  $q$  are derived from sets of spectra measured over different temperature ranges. There is no way to know *a priori* whether a change in the shape of  $\Phi_q(\bar{t})$  is due to decreasing  $q$  or to increasing  $T$ . Experimentally, this difficulty could only be overcome if it were possible to significantly ameliorate the energy resolution of quasielastic small-angle scattering.

At present, we must rely on an analogy: In our CNS study of glycerol [16] we found that the Kohlrausch exponent depends only weakly on temperature increasing by not more and probably much less than 0.15 over the same temperature interval 270–413 K covered in the present INS work. This suggests that also the INS relaxation curves depend only weakly on temperature, and that at a given temperature the line shapes do indeed cross over from stretched exponential to single exponential behavior.

Stronger conclusions can be drawn on behalf of the wave-number dependence of  $\langle \tau_q \rangle$ . From our simulation as well as from the analytic argument based on Eq. (8) we know that multiple scattering has negligible influence upon the experimental determination of  $\langle \tau_q \rangle$ . Also a large uncertainty in the stretching exponent  $\beta_q$  only weakly affects the fitted value of  $\langle \tau_q \rangle$ . The only assumption that seriously enters our determination of  $\langle \tau_q(300 \text{ K}) \rangle$  is the viscosity scaling (3). This assumption can be justified by fits to our NMR data: Down to at least 260 K we find

$$D^{-1} = q^2 \langle \tau_q \rangle \propto \eta / T \quad (9)$$

within the precision of available viscosity data [20].

So we can conclude that up to wave numbers of about 0.2 or  $0.3 \text{ \AA}^{-1}$  the relaxation time does indeed follow the hydro-

dynamic  $q^{-2}$  law (7), while for larger  $q$  it decreases definitely stronger than that. A similar deviation from diffusional wave-number dependence has been observed in a number of other glass formers [18,23], and it has been suggested that the relaxation time follows a power law  $\langle \tau_q \rangle \propto q^n$  with an exponent related to the Kohlrausch parameter through  $n = -2/\beta$ . A fit to our INS data shows that such a power law holds in glycerol at best in quite a small transitory region. Our results rather suggest that once  $\langle \tau_q \rangle$  deviates from  $q^{-2}$ , its further  $q$  dependence cannot be parametrized by just one overall exponent  $\beta$ .

So both the line shape of the self-correlation master curve and the mean relaxation time indicate that tagged-particle motion resembles Brownian diffusion down to a crossover wave number of the order of  $0.2 \text{ \AA}^{-1}$ , where coupling to structural relaxation sets in. Physically, such a behaviour is quite plausible. While normal diffusion leads to an exponential decay of correlations (5) a stretched exponential function reveals memory effects. In contrast to a Brownian particle that performs an uncorrelated random walk, the motion of a tagged particle in a dense liquid depends on its history. When a particle is trapped in a given surrounding, each step out of the cage will be followed by an increased probability that the next step is in the backward direction. The typical time it takes to escape from a local cage may be roughly estimated from the mean relaxation time  $\langle \tau_q \rangle$  at about the structure factor maximum. It seems then reasonable that after some ten escapes the particle has lost any memory of its initial position and that for longer times its motion resembles ordinary diffusion.

While normal diffusion implies a  $q^{-2}$  dependence of  $\langle \tau_q \rangle$ , no generic predictions can be made for correlated motion. This view is also taken by mode-coupling theory: Integrating the long-time limit of the equation of motion [24], we find

$$\langle \tau_q \rangle = D_q^{-1} f_q^{-1} q^{-2}, \quad (10)$$

where  $f_q$  is the amplitude of structural relaxation and  $D_q$  is a  $q$ -dependent generalization of the diffusion constant. For the special case of a hard-sphere system, the product  $D_q^{-1} f_q^{-1}$  was found to be constant up to wave numbers above the structure factor maximum [24]. It cannot be expected that the same cancellation in the  $q$  dependence of  $f_q$  and  $D_q$  occurs also in more complex liquids, the structure of which cannot be modeled by hard spheres. So mode-coupling theory makes it plausible that  $\langle \tau_q \rangle$  deviates from  $q^{-2}$  as soon as one approaches microscopic length scales where  $f_q$  and  $D_q$  begin to vary with  $q$ .

## VI. CONCLUSION

To summarize, we have combined incoherent neutron scattering and field gradient NMR measurements to yield the self-correlation function of a viscous liquid for microscopic and mesoscopic wave numbers. The broad  $q$  range allowed us to distinguish two limiting regions: For small wave numbers, one observes ordinary Brownian diffusion; for wave numbers around the structure factor maximum, tagged-particle motion is strongly coupled to the collective process of structural relaxation.

An extensive multiple-scattering simulation was performed to find out how far the quasielastic spectra can be trusted, particularly at small wave numbers. In a master curve analysis, we could discern clear signs of a crossover between relaxationlike and diffusionlike motion: At  $q \leq 0.3 \text{ \AA}^{-1}$ , the self-correlation function shows typical relaxational stretching at short times, while for long times its decay becomes exponential. At about the same wave number, mean relaxation times begin to deviate from the hydrodynamic  $q^{-2}$  behavior. For larger  $q$ , the wave-number dependence seems to be nongeneric.

A simple interpretation can be given if particle trajectories are considered: The characteristic time of structural rear-

rangements can be taken from coherent scattering at the structure factor maximum. It is then plausible that a tagged particle conserves a strong memory of several rearrangement steps, whereas for longer times it performs an uncorrelated random walk.

#### ACKNOWLEDGMENTS

We acknowledge support by the Deutsche Forschungsgemeinschaft through Sonderforschungsbereich 262 and by Bundesministerium für Bildung und Forschung under Teilprojekt 03PE4TUM9. We thank W. Götze for a critical reading of the manuscript.

- 
- [1] W. Marshall and S. W. Lovesey, *Theory of Thermal Neutron Scattering* (Clarendon, Oxford, 1971).
- [2] J. P. Boon and S. Yip, *Molecular Hydrodynamics* (McGraw-Hill, New York, 1980).
- [3] P. A. Egelstaff, *An Introduction to the Liquid State* (Clarendon, Oxford, 1992).
- [4] K. Sköld, J. M. Rowe, G. Ostrowski, and P. D. Randolph, *Phys. Rev. A* **6**, 1107 (1972); C. Morkel and W. Gläser, *ibid.* **33**, 3383 (1986).
- [5] W. Götze and A. Zippelius, *Phys. Rev. A* **14**, 1842 (1974); U. Balucani, A. Torcini, A. Stangl, and C. Morkel, *Phys. Scr.* **T57**, 13 (1995).
- [6] See Ref. [16] for an exhaustive list of references.
- [7] J. Wuttke, J. Hernandez, G. Li, G. Coddens, H. Z. Cummins, F. Fujara, W. Petry, and H. Sillescu, *Phys. Rev. Lett.* **72**, 3052 (1994).
- [8] J. Wuttke, W. Petry, G. Coddens, and F. Fujara, *Phys. Rev. E* **52**, 4026 (1995).
- [9] E. Rössler, A. P. Sokolov, A. Kisliuk, and D. Quitmann, *Phys. Rev. B* **49**, 14 967 (1994).
- [10] W. Götze, in *Liquids, Freezing and the Glass Transition*, Proceedings of the Summer School of Theoretical Physics, Les Houches, 1989, Session LI, edited by J. P. Hansen, D. Levesque, and D. Zinn-Justin (North-Holland, Amsterdam, 1991); W. Götze and L. Sjögren, *Transp. Theory Stat. Phys.* **24**, 801 (1995).
- [11] F. Fujara and W. Petry, *Europhys. Lett.* **4**, 921 (1987); W. Knaak, F. Mezei, and B. Farago, *ibid.* **7**, 527 (1988); W. Petry and J. Wuttke, *Transp. Theory Stat. Phys.* **24**, 1075 (1995).
- [12] N. J. Tao, G. Li, and H. Z. Cummins, *Phys. Rev. Lett.* **66**, 1334 (1991); H. Z. Cummins, G. Li, W. M. Du, J. Hernandez, and N. J. Tao, *Transp. Theory Stat. Phys.* **24**, 981 (1995).
- [13] G. Fleischer and F. Fujara, in *NMR—Basic Principles and Progress, Vol. 30*, edited by P. Diehl, E. Fluck, H. Günther, R. Kosfeld, and J. Seelig (Springer, Berlin, 1994).
- [14] I. Chang, F. Fujara, B. Geil, G. Hinze, H. Sillescu, and A. Tölle, *J. Noncryst. Solids* **172–174**, 674 (1994).
- [15] I. B. Rabinovich, V. I. Murzin, and L. S. Zhilkin, *Zh. Fiz. Khim.* **34**, 1973 (1960).
- [16] J. Wuttke, S. Pouget, and W. Petry, *J. Chem. Phys.* (to be published).
- [17] F. Mezei, W. Knaak, and B. Farago, *Phys. Scr.* **T19**, 363 (1987); D. Richter, B. Frick, and B. Farago, *Phys. Rev. Lett.* **61**, 2465 (1988); E. Bartsch, O. Debus, F. Fujara, M. Kiebel, W. Petry, H. Sillescu, and J. H. Magill, *Physica B* **180–181**, 808 (1992); C. Simon, G. Faivre, R. Zorn, F. Batallan, and J. F. Legrand, *J. Phys. (France) I* **2**, 307 (1992).
- [18] W. Petry, E. Bartsch, F. Fujara, M. Kiebel, H. Sillescu, and B. Farago, *Z. Phys. B* **83**, 175 (1991).
- [19] F. Fujara, *J. Mol. Struct.* **296**, 285 (1993).
- [20] V. Vand, *Research* **1**, 44 (1947); J. B. Segur and A. E. Oberstar, *Ind. Eng. Chem.* **43**, 2117 (1951); R. Piccirelli and T. Litovitz, *J. Acoust. Soc. Am.* **29**, 1009 (1957).
- [21] J. Wuttke, M. Kiebel, E. Bartsch, F. Fujara, W. Petry, and H. Sillescu, *Z. Phys. B* **91**, 357 (1993).
- [22] J. R. D. Copley, *Comput. Phys. Commun.* **7**, 289 (1974).
- [23] J. Colmenero, A. Alegría, A. Arbe, and B. Frick, *Phys. Rev. Lett.* **69**, 478 (1992); J. Colmenero, A. Arbe, and A. Alegría, *J. Noncryst. Solids* **172–174**, 229 (1994).
- [24] M. Fuchs, I. Hofacker, and A. Latz, *Phys. Rev. A* **45**, 898 (1992).